

Thermal, Mechanical, and Rheological Properties of Plasticized Poly(L-lactic acid)

Huanhuan Ge,¹ Fan Yang,¹ Yanping Hao,¹ Guangfeng Wu,¹ Huiliang Zhang,² Lisong Dong²

¹Engineering Research Center of Synthetic Resin and Special Fiber, Ministry of Education, Changchun University of Technology, Changchun 130012, China

²Key Laboratory of Polymer Ecomaterials, Chinese Academy of Sciences, Changchun Institute of Applied Chemistry, Changchun 130022, China

Correspondence to: H. Zhang (E-mail: hlzhang@ciac.jl.cn)

ABSTRACT: Polylactide (PLA) is an attractive candidate for replacing petrochemical polymers because it is biodegradable. In this study, a specific PLA 2002D was melt-mixed with a new plasticizer: glycerol monostearate (GMS). The PLA/GMS blends with different ratios were analyzed by dynamic mechanical analysis and differential scanning calorimetry. Although a slightly phase separation can be seen in DSC curves, the SEM micrographs of the impact fracture surfaces of PLA/GMS blends had a relatively good separation and this phenomenon was in good agreement with their higher impact strength. The result showed that the adding of GMS has enhanced the flexibility of PLA/GMS blends as compared to neat PLA. The relationship between complex viscosity and angular frequency of the PLA/GMS blends exhibits that the melt viscosity substantially lower than that of neat PLA. For example, at 10 rad/s, the melt viscosity of PLA/GMS (85/15) was reduced by about 7.2% compared to that of neat PLA. The impact strength was changed from 4.7 KJ/m² for neat PLA to 48.2 KJ/m² for 70/30 PLA/GMS blend. © 2012 Wiley Periodicals, Inc. *J. Appl. Polym. Sci.* 000: 000–000, 2012

KEYWORDS: polylactide; thermal properties; mechanical properties; plasticizer; differential scanning calorimetry (DSC)

Received 13 January 2012; accepted 29 February 2012; published online

DOI: 10.1002/app.37620

INTRODUCTION

In today's society, the rapid growth of municipal waste has become more and more serious. Polymeric materials constitute a large part of the waste and cannot be recycled. It is in many ways similar to poly(ethylene terephthalate). Consumer awareness in conjunction with strict laws and regulations has emphasized the demand to develop biologically degradable plastics and products that may be composted.

Biodegradable polymers that are produced from renewable raw materials have many advantages. On degradation, they do not give any net contribution to the carbon dioxide emissions in the atmosphere. Also, because they are based on agricultural products such as whey, corn, potato, and molasses, crude oil resources are saved. Biodegradable polymers offer new possibilities for use of agricultural products, which especially in the developed countries, suffer from overproduction.

Poly(lactic acid) (PLA) is undoubtedly one of the most promising polymers for further developments because it is not only biodegradable but also produced from renewable resources, like sugar beets or corn starch.^{1–3} Thus, PLA were initially investi-

gated for drug delivery, suture and orthopedic implant applications.^{4–12} Considering of its good properties, such as high elasticity modulus, high stiffness, thermoplastic behavior, and processability using most conventional techniques and equipment,^{13,14} PLA would be a good candidate to produce biodegradable packaging and hygiene products. As a result, the environment would benefit greatly if PLA could be used in household applications. However, the inherent high modulus and low elongation at break have been the major drawbacks and limited its application only to the rigid thermoformed packing industry whereas for flexible packaging new grades of PLA with specific end-use performances are required.

Several attempts have been proposed to improve the mechanical properties of PLA, such as copolymerization with other monomers, polymer blending and the use of plasticizer. The method of copolymerization processes have been proved not economically viable and the copolymers can not be produce on an industrial scale for packaging applications.^{15–18} Blending PLA with other biodegradable polymers or copolymers has also been widely investigated to prepare soft or more flexible materials for many different applications. To easily achieve

© 2012 Wiley Periodicals, Inc.

property modulation, the crucial point seems to be the miscibility and compatibility between the phases. However, in fact, all of the investigated biodegradable polyesters, including poly(ethylene succinate),¹⁹ poly(hydroxyl butyrate),²⁰ poly(butylene succinate),²¹ polycaprolactone,^{22,23} and poly(butylene adipate-co-terephthalate) (PBAT),^{24,25} are immiscible with PLA. The latter allowed the preparation of materials with interesting mechanical properties, for example a good level of toughness.²⁶ Because of the final properties of the obtained blends depend on many respects, such as the composition, level of compatibility, processing, and morphological features, PLA can only achieve moderate improvement through the blending approach. Consequently, we could choose the way of finding suitable plasticizers. The choice of plasticizers to be used as modifiers for PLA is limited by the requirement of the application. First, the plasticizing agent used in food packaging materials must be non-toxic substances approved for food contact. Second, the plasticizer should be compatible with PLA and stable at the elevated temperature used during processing. Third, the PLA/plasticizer blends should be stable over time because the migration of the plasticizer to the surface could be a source of contamination of the food or beverage in contact with the packaging or may possibly regain the initial brittleness of pure PLA.

In past decades, a large amount of research was aimed at the plasticization of PLA to produce flexible films. Poly(ethylene glycol) was found to be a good plasticizer, because PEG has good miscibility with PLA even with a low molecular weight. Blending PLA with PEG can drastically lower the T_g of PLA and create homogeneous and flexible materials. However, the promising mechanical properties of PLA/PEG blends disappeared with time because of their slowly phase separation and the crystallization of PEG at the room temperature.²⁷ In this study, GMS is a new plasticizer to PLA. The addition of GMS can reduce the T_g and T_c of the PLA, and the impact strength was changed significantly from 4.7 KJ/m² for neat PLA to 46.1 KJ/m² for PLA/GMS blend with the ratio of 75/25. Although a slightly phase separation can be seen in the SEM micrographs of the impact fracture surfaces, the PLA/GMS blends had a relatively good separation and this result was in good agreement with their higher impact strength.

EXPERIMENTAL

Materials

Semi-crystalline PLA Grade 2002D (4% D-lactide, 96% L-lactide content, molecular weight 121,400 g/mol, MFR 6.4 g/10 min) was obtained from Nature worksTM in pellet form. Glycerol Monostearate (GMS) (Henan Zhengtong Chemical Co., Ltd, China), the GMS had a molecular weight of 358 g/mol and a melting point of 44°C.

Sample Preparation

Before blending, all polymers were dried in vacuum at 50°C for 24 h. Blends of PLA/GMS was prepared by melt mixing using a twin screw Haake Reomix 600 at 60 rpm and 180°C for 5 min. The mixing compositions of the blends were 95/5, 90/10, 85/15, 80/20, 75/25, and 70/30 w/w. After blending, all the samples were cooled to room temperature under atmosphere air. Also,

the neat PLA was subjected to the same mixing treatment so as to obtain a reference material. Films were prepared using a hot press at 180°C, a hold pressure of 6 MPa and a hold time of 3 min, followed by quenching to room temperature between two thick-metal blocks kept at room temperature. The blocks were cooled on a large metal plate in the air for about 10 min between each quenching round to keep the same processing temperature. A template frame was used to ensure a constant film thickness of 4.0 mm for impact test and 1.0 mm for tensile test, and care was taken to ensure the same thermal history of all films. The specimens were then sealed in plastic bags awaiting the processing and analysis.

CHARACTERIZATION

Mechanical Properties Testing

Notched Izod impact tests were performed at 23°C ± 2°C according to ASTM D256 on an impact testing machine (CEAST, Chengde, China). The samples with dimensions 63.2 × 12.0 × 4.0 mm³ were obtained from compression-molded specimens. The notch was milled in having a depth of 2.54 mm, an angle of 45°, and a notch radius of 0.25 mm. The uniaxial tensile tests were carried out at 23°C ± 2°C on an Instron 1121 testing machine (Canton, MA). Specimens (20 × 4 × 1 mm³) were cut from the previously compression-molded sheet into a dumbbell shape. The measurements were conducted at a cross-head speed of 50 mm/min at room temperature according to ASTM D638. At least five runs for each sample were measured, and the results were averaged.

Dynamic Mechanical Properties Testing

Dynamic mechanical analysis was performed on a NETZSCH DMA 242C (Selb, Germany), which provided the plots of the loss tangent (tan δ) and the storage modulus (E') against temperature. The samples were sized 20 × 4 × 1 mm³. The experiment was carried out in tension mode at a constant heating rate of 3°C/min and a frequency of 3.33 Hz, from -60 to 180°C.

Differential Scanning Calorimetry

Crystallization behavior of the composites was studied by differential scanning calorimetry (DSC; TA Instruments DSC Q20) on the specimens sliced from compression molded samples. The heating and cooling rates were 10°C/min with nitrogen purge, and the sample weights were between 8 and 10 mg. The samples were heated first from 20 up to 180°C at 10°C/min and held at 180°C for 5 min to eliminate their previous thermal history, then cooled at the same rate and heated again finally. The absolute degree of crystallinity [$X(t)$] of the samples was evaluated from the heat evolved during crystallization by the following relationship:

$$X(t) = \left[\int_{t_0}^t (dH/dt) \right] / (1 - \Phi) \Delta H_f^0 \quad (1)$$

where ΔH_f^0 is the heat of fusion for 100% crystalline PLA (93 J/g) and Φ is the weight fraction of GMS in the blend system.

Rheological Behaviors Testing

Rheological measurements of the blends were carried out on a Physica MCR 2000 rheometer (AR 2000ex). Frequency sweep

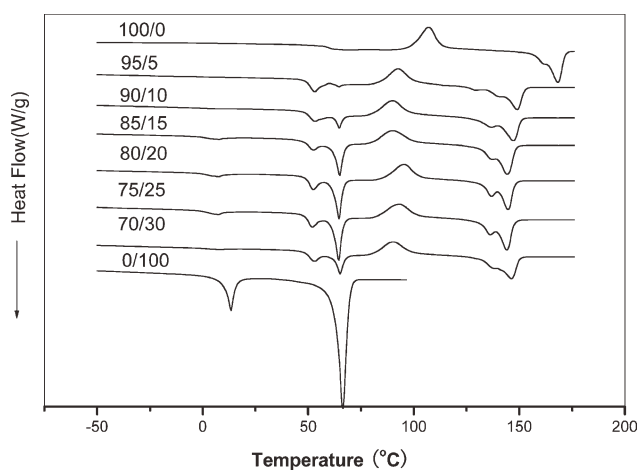


Figure 1. DSC thermograms for PLA/GMS blends with compositions from 100/0 to 0/100.

for the PLA/GMS samples was carried out under nitrogen using 25-mm plate-plate geometry. The gap distance between the parallel plates was 0.8 mm for all tests. The sheet samples were about 1.0 mm in thickness. A strain sweep test was initially conducted to determine the linear viscoelastic region of the materials. The angular frequency range used during testing was 0.1–100 rad/s. The temperatures were plotted at 170°C.

Morphological Characterization

The PLA/GMS polyblend the sculpture 4 h later quenches absolutely the surface SEM picture through the normal temperature under the ethyl alcohol solution. The cryogenically fracture surfaces and the Izod-fracture surfaces of PLA/GMS blends were characterized by SEM (model Japan JXA-840 ESEMFE), respectively. A layer of gold was sputter-coated uniformly over all of the fractured surfaces before SEM observations.

RESULT AND DISCUSSION

Thermal Characterization of PLA Blends

In the PLA/GMS blends, the effect of GMS on the thermal behavior of PLA is connected with the mechanical properties of

the blends. Figure 1 shows the secondary warming curves of the pure PLA and the blends, and the specific thermodynamic parameters are listed in Table I. The samples are through the same treatment, so they have the same thermal history. That is to say, all samples are heated up from amorphous state.

Figure 1 shows the thermal response of the samples with the increasing of temperature. First, there is the transition from glass state to high-elastic state. The characteristic temperature is the glass transition temperature (T_g); the cold crystallization behavior was appeared with increasing temperature, and the corresponding peak value and enthalpy are expressed by T_{cc} and ΔH_{cc} . After increasing temperature, samples are melted, and present contiguous double peaks, corresponding to T_{m1} and T_{m2} , and molten enthalpy is ΔH_m .

Table I shows the decreases of the T_g of the PLA in blends, and this attributes to the lubrication action of GMS. The GMS micromolecule can permeate into the inside of PLA molecule, increase the lubricity of the molecule, decrease the resistance deformation of interior, overcome the adhesive force that created by the strong van der Waals force and hydrogen bond of PLA molecule, which increases the flexibility and impact strength of materials. There is another reason must to say that is free volume effect. Because of the decrease of molecular stack density, which causes by the quite low molecular weight and may chain end, the additional free volume is decreasing that render the decreasing of the glass transition temperature and increasing molecular chain flexibility.

In Figure 1 pure PLA appears an exothermic peak on 108°C, which proves that PLA has the ability of cold crystallization. However, the cold crystallization peaks of PLA/GMS blends are moved to low temperature, which indicated clearly that GMS has the ability to enforce the cold crystallization of PLA. This phenomenon can be attributed to the smaller molecular chain binding, which generated by GMS. In the PLA/GMS blends, the lowest T_{cc} is 89.7°C, corresponding to 10 wt % GMS content. T_{cc} moves to higher temperature when GMS content exceeds 10 wt %. That is because of the agglomeration of GMS, which acted negative effect on the crystallization of PLA (shown in SEM).

Table I. Thermal Properties of PLA/GMS Blends

PLA/GMS (w/w)	Second heating run									
	T_{m1} (°C)	T_{m2} (°C)	T_{m3} (°C)	T_{g1} (°C)	T_{g2} (°C)	T_{cc} (°C)	ΔH_{cc} (J/g)	ΔH_m (J/g)	ΔH_f (J/g)	X_c (%)
100/0	168.2	—	—	58.6	—	122.4	—	—	5.7	6.2
95/5	148.9	140.2	63.7	52.7	—	92.7	21.8	29	31.9	36.1
90/10	147.2	136.5	65.4	52.5	—	89.7	22	31.8	30.6	36.5
85/15	146.2	135.9	66	52.3	6.9	89.9	17.6	27.6	29.5	37.3
80/20	144.2	135.8	65.7	51.9	7	89.8	18.5	32.1	33.9	45.6
75/25	144.6	135.3	65.3	52.1	7.1	95.1	18.8	29.6	30.6	43.9
70/30	144.1	136	65.2	51.5	7.2	92.8	18.5	31.6	34	52.2
0/100	—	—	66.2	—	12.8	—	—	—	—	—

Thermal properties of PLA/GMS blends.

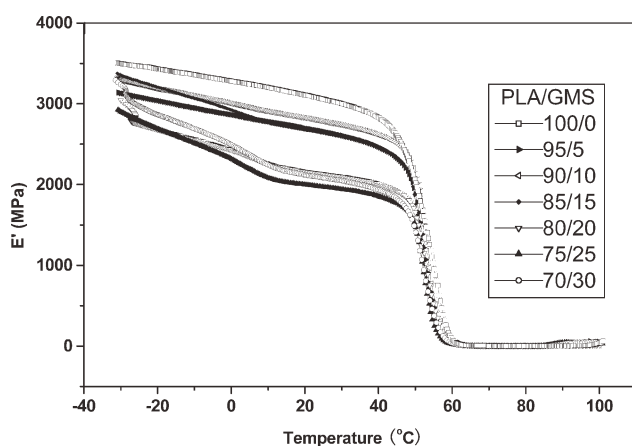


Figure 2. Dynamic mechanical properties of PLA/GMS blends: the storage modulus.

The obvious change of T_m also indicates the plastic function of PLA. The T_m of PLA/GMS blends are far below the pure PLA. Besides, the molten peak is changed from one to two. That probably attributes to secondary crystallization. GMS make the crystallization of PLA faster, decreased the spherocrystal perfect degree, which engenders these crystal grain that has not perfect crystallization come into secondary crystallizing after melting in the process of heating up. Similarly performance of double peaks also reported in other PLA blending systems.

DMA experiments were carried out on most PLA/GMS blend series. Exemplary temperature dependencies of the storage modulus and $\tan \delta$ for the blends studied are plotted in Figures 2 and 3.

It can be seen that the drop in storage modulus (Figure 2) occurs at a lower temperature for the blends as compared with neat PLA. But the E' shows only a slight dependence on the composition.

The glass transition reflected in the $\tan \delta$ peaks is followed by cold crystallization of the amorphous materials. The plasticization decreased temperatures of both transitions to lower temperature, which was not clearly shown in DMA thermograms. The $\tan \delta$ curves showed a sharp peak around 62°C and a peak at high temperature (about 95°C) of the PLA/GMS blends, which is associated with the α -relaxation and the cold crystallization. But the result was not consistent with the data of DSC.

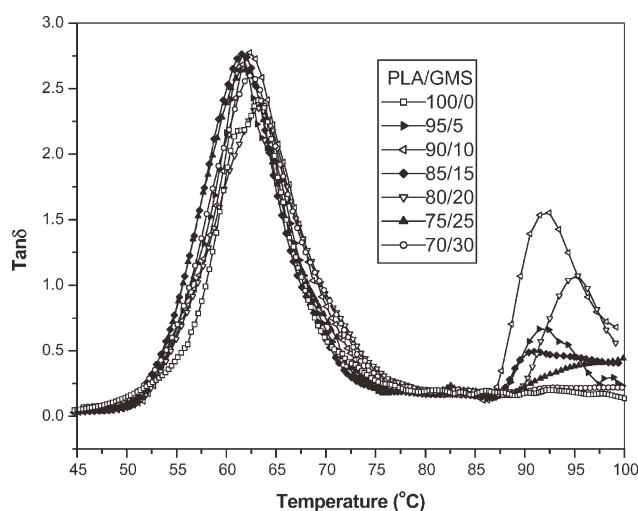


Figure 3. Dynamic mechanical properties of PLA/GMS blends: $\tan \delta$.

Mechanical Characterization of PLA Blends

The mechanical properties (tensile strength and impact strength) of PLA/GMS blends, as well as those of pure components, are shown in Table II.

The goal of adding plasticizer to PLA is to enhance plastic elongation and reduce brittleness and at the same time maintaining maximum polymer strength and stiffness. The stress–strain curves of neat PLA and PLA/GMS blends are shown in Table II. Table II presents the Young's modulus, tensile strength, elongation at break and Izod impact strength. It can be seen that neat PLA and 95/5 PLA/GMS blend are fractured at low strain before yielding, whereas the 90/10, 85/15, 80/20, 75/25, and 70/30 PLA/GMS blends exhibited a ductile behaviour with yielding and a subsequent plastic deformation. The neat PLA presented high Young's modulus and tensile strength at 1777 MPa and 70 MPa, respectively, and a relatively low elongation at break, around 6%. The plasticizer increases the ability of PLA to plastic deformation which is reflected in the decrease of Young's modulus and tensile strength, and in an increase of elongation at break. The decrease of the tensile strength is quite well correlated with the percentage of plasticizer. When the content of the PLA/GMS blends was 95/5 or 90/10, the Young's modulus and tensile strength had a slightly decrease, whereas the elongation at break shown a slightly increase. For example, the 90/10 PLA/GMS blends presented Young's modulus and tensile strength at 1200 MPa and 42 MPa,

Table II. Mechanical Properties of PLA/GMS Blends

PLA/GMS (w/w)	Young's modulus (MPa)	Tensile strength (MPa)	Elongation at break (%)	Izod impact Strength (kJ/m ²)
100/0	1777 ± 42	69.8 ± 3.2	5.7 ± 0.3	4.7 ± 0.2
95/5	1570 ± 44	44.8 ± 1.3	4.5 ± 0.5	8.1 ± 0.4
90/10	1200 ± 12	41.9 ± 4.6	7.6 ± 2.4	8.5 ± 0.5
85/15	1270 ± 36	39.7 ± 1.0	11 ± 5.0	15.5 ± 0.3
80/20	1210 ± 17	35.1 ± 2.1	9.5 ± 6.5	36.7 ± 0.3
75/25	1190 ± 24	32.4 ± 1.8	11 ± 3.1	46.1 ± 2.9
70/30	695 ± 38	29.9 ± 2.6	45 ± 15.8	48.2 ± 4.6

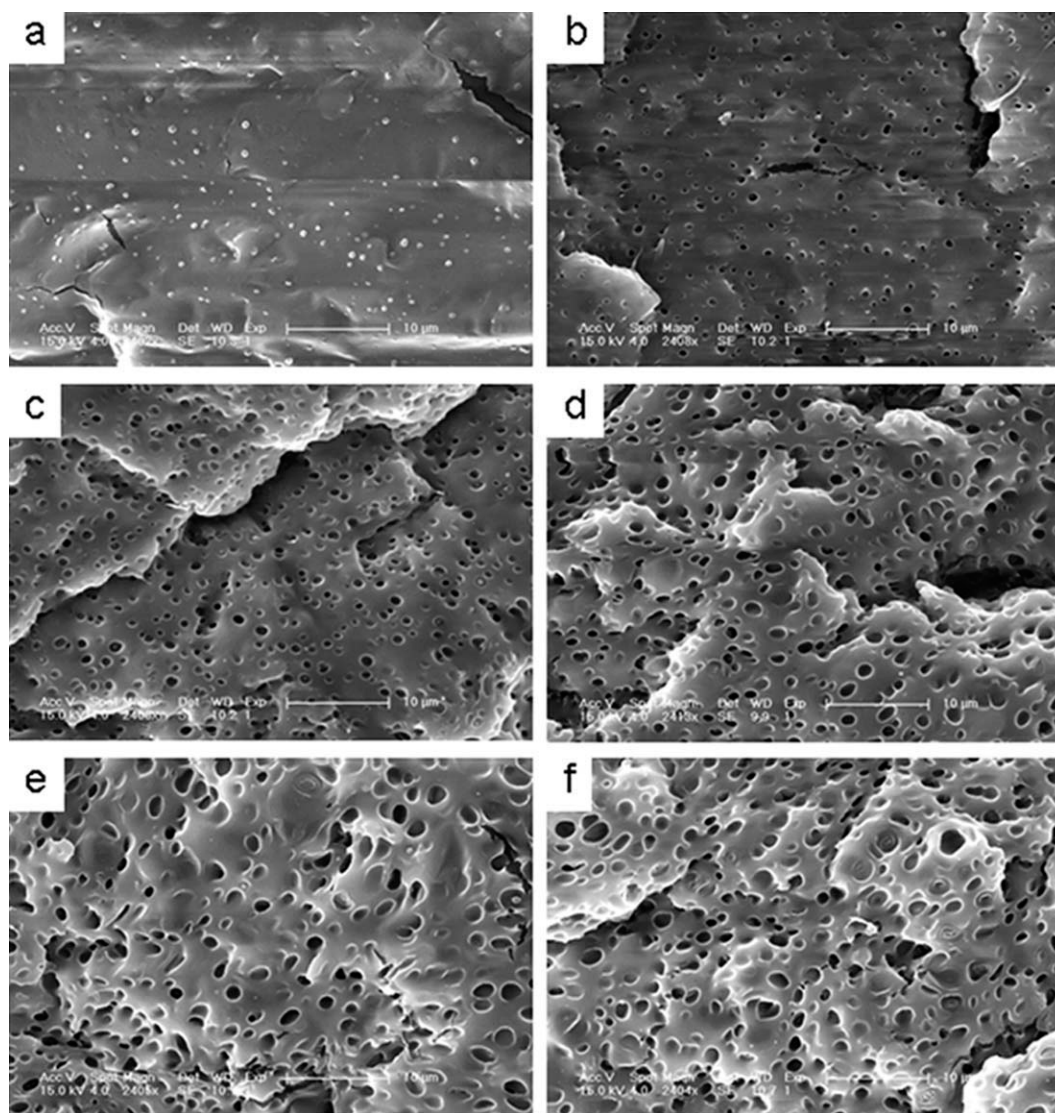


Figure 4. SEM micrographs of the impact fracture surfaces of amorphous PLA/GMS blends: (a) 95/5, (b) 90/10, (c) 85/15, (d) 80/20, (e) 75/25, and (f) 70/30.

respectively, and the elongation at break around 8%. When the content of the PLA/GMS blends was 70/30, the Young's modulus and the tensile strength reached to 695 MPa and 30 MPa, respectively. Conversely, the elongation at break shown a most increase into 45% compared with neat PLA.

From Table II, the impact strength was changed significantly from 4.7 KJ/m² for neat PLA to 46.1 KJ/m² for the 75/25 PLA/GMS blend. The brittle-ductile transition of the blends was obtained when the GMS content varied from 15% to 20%. It was found that the PLA/GMS blends exhibited inferior tensile

strength as compared with the PLA matrix, but superior toughness from the mechanical properties. PLA had been toughened by GMS. The mechanical properties may be explained in terms of the slightly compatibility between the two phases.

The PLA/GMS polyblend the sculpture 4 h later quenches absolutely the surface SEM picture through the normal temperature under the ethyl alcohol solution. Sea-island liked structure is observed in the impact fracture surface of PLA/GMS blends: (a) 95/5, (b) 90/10, (c) 85/15, (d) 80/20, (e) 75/25, and (f) 70/30.

Table III. The Average Particle Sizes and Partied Size Distribution of PLA/GMS Blends

GMS weight content (%)	5	10	15	20	25	30	5
GMS volume content (%)	5.2	10.3	15.5	20.6	25.8	30.9	5.2
Particle size (μm)	0.44	0.52	0.7	0.92	1.17	1.19	0.44
Polydispersity σ	1.38	1.35	1.24	1.28	1.26	1.28	1.38

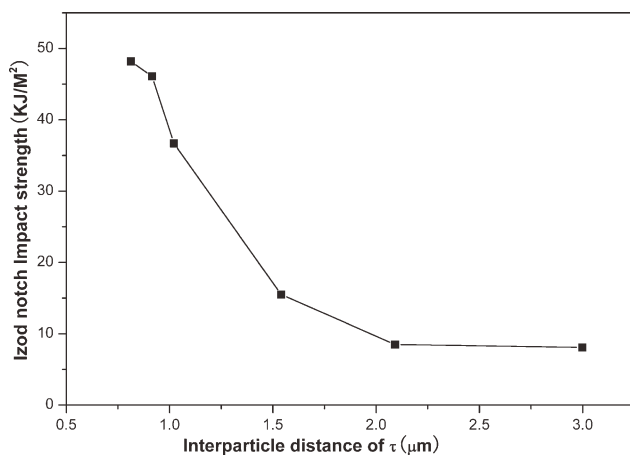


Figure 5. The impact strength as a function of inter-particle distance of PLA/GMS blends.

The addition of plasticizer GMS promotes the aggregated PLA particles to separate from each other during blending. Meanwhile, the GMS permeates into the PLA particles and the PLA molecules tend to disentangle and separate from each other due to the enhanced mobility of PLA chain caused by the plasticization of GMS. This phenomenon can be seen in the rheology analysis.

A brittle–ductile transition has been observed in many blend toughened system. Wu^{28,29} suggested that the inter-particle distance is the primary controlling factor for toughening in polymer blends. Wu also indicated that if the inter-particle distance is below the critical value, then the blend will be tough; if the inter-particle distance is above the critical value, the blend will be brittle. For PLA/GMS blends, filler dispersions are studied by SEM (Figure 4) and the distribution in particle size is quantified by image analysis.

Considering the actual situation, the particle sizes of the blends frequently obey a log-normal distribution.³⁰ The average inter-particle distance (τ) for the blend can be calculated from the equation³¹:

$$\tau = d[(\pi/6V_f)^{1/3} \exp(1.5\ln^2\sigma) - \exp(0.5\ln^2\sigma)] \quad (2)$$

where d is the number average particle diameter, V_f is volume fraction of these particles, and σ is particle size distribution. Equation (2) shows that when the size distribution is polydisperse, τ is not defined by d and V_f alone. It also depends significantly on the width of the size distribution represented by parameter σ . Using the parameter listed in Table III, the inter-particle distance can be worked out through eq. (2). A rather good correlation between impact strength and inter-particle distance by changing the content of fillers is described in Figure 5. A brittle-to-ductile transition marking the onset of toughening efficiency occurs around a critical inter-particle distance, τ_c of about 1.5 μm . Below this critical value, high toughness levels are achieved: the impact strength is increased from 4.7 KJ/m^2 for pure PLA up to about 48.2 KJ/m^2 with 30 phr GMS particles.

Rheological Measurement Results

Oscillatory measurement is the most common dynamic method to study the viscoelastic behavior of any material. The rheo-

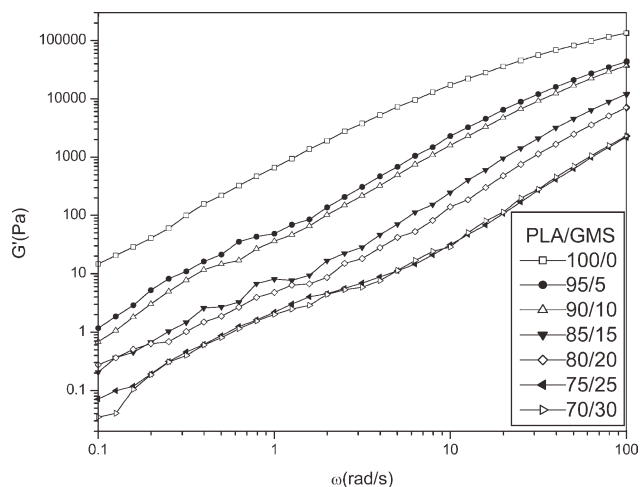


Figure 6. Plots of storage modulus versus angular frequency for the PLA and PLA/GMS blends measured at 170°C.

grams of dynamic storage modulus G' , dynamic loss modulus G'' , and complex viscosity η^* versus oscillatory frequency were prepared by conducting dynamic frequency sweep test ($\omega = 0.1$ –100 rad/s) on the blends at the temperature of 170°C, as shown in Figures 6–8. Figure 6 displayed the relationship between storage modulus and angular frequency of the PLA/GMS blends. It could be seen that the G' of PLA/GMS blends increased with angular frequency, but decreased with the increase of GMS content in the blends. The possible reason for increase in mechanical strength (G') of PLA/GMS blends over neat PLA could be the lower elasticity of GMS. The lower storage modulus of the blends is supposed to be originated from the decrease in molecular entanglements in the blends.

Figure 7 displays the relationship between loss modulus and angular frequency of the PLA/GMS blends. It can be seen that the loss modulus of PLA blends increases with angular frequency. At the whole frequency, the G'' of PLA/GMS blends were much lower than that of neat PLA. The much lower G'' indicated lower viscosity. The G'' of PLA/GMS decreased with

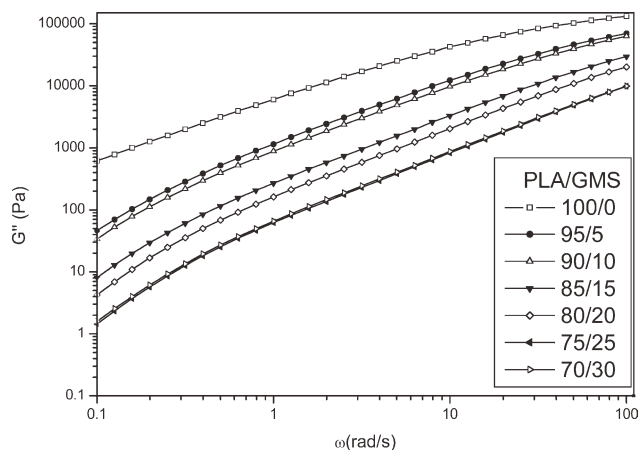


Figure 7. Plots of loss modulus versus angular frequency for the PLA and PLA/GMS blends measured at 170°C.

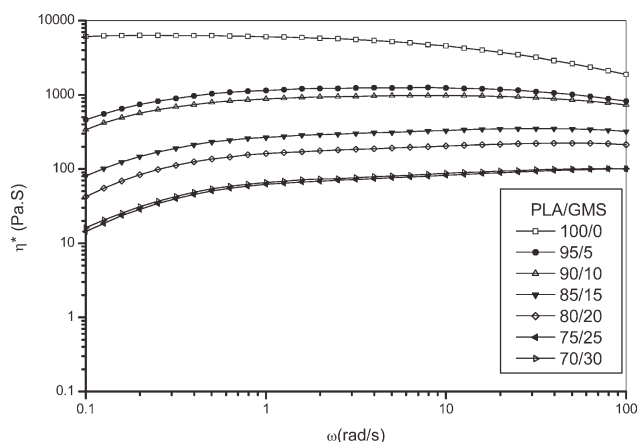


Figure 8. Plots of complex viscosity versus angular frequency for the PLA and PLA/GMS blends measured at 170°C.

the increase of GMS content in the blends. The neat PLA was a stiff, relatively brittle polymer. Addition of GMS improved the ductility dramatically. As expected, the low molecular weights GMS acts as an effective plasticizer and lowered both elastic and viscous moduli drastically.

The melt viscosity of polymers is very sensitive to changes in the macromolecular chain structure and to the addition of plasticizers which by definition increases the polymer free volume and the polymer chains' mobility. Therefore, the rheology is of practical and fundamental interest in the current study.

Figure 8 presented the relationship between complex viscosity and angular frequency of the PLA/GMS blends. It exhibits that the melt viscosity of the blends are substantially lower than that of neat PLA. For example, at 10 rad/s, the melt viscosity of the PLA/GMS (85/15) was reduced by about 7.2% compared to that of neat PLA. Neat PLA melt showed non-Newtonian behavior at high frequency region. The 85/15, 80/20, 75/25 PLA/GMS blends exhibit a more pronounced Newtonian response with an extended Newtonian plateau compared with neat PLA. The decreased melt viscosity of the blend can be related to an increased free volume due to the plasticization by GMS.

CONCLUSIONS

In this study, a new plasticizer (GMS) was added to PLA matrix with different ratios, such as 95/5, 90/10, 85/15, 80/20, 75/25, and 70/30, for improving the flexibility of neat PLA.

The addition of plasticizers increases the polymer free volume and improves the polymer chains' mobility. The PLA/GMS blends exhibit that the melt viscosity is substantially lower than that of neat PLA. For example, at 10 rad/s, comparing to the melt viscosity of neat PLA, the PLA/GMS (85/15) was reduced by about 7.2%. The 85/15, 80/20, and 75/25 PLA/GMS blends exhibit a more pronounced Newtonian response with an extended Newtonian plateau. Because of the plasticization effect of GMS, the melt viscosity of the blends decreased and this phenomenon can be related to an increased free volume.

The addition of GMS can also reduce the T_g , T_m , and T_c of the PLA. The decrease of T_g shows the effect of the GMS in PLA

compositions with increasing molecular mobility. Although a slightly phase separation can be seen in the DSC curves and SEM micrographs, the PLA/GMS blends had a relatively good separation. This can be also seen in the result of the impact strength. For example, the impact strength was changed significantly from 4.7 KJ/m² for neat PLA to 48.2 KJ/m² for the 70/30 PLA/GMS blend. Therefore, both the thermal stability and the mechanical property of PLA were simultaneously improved by the use of GMS.

ACKNOWLEDGMENTS

This work was supported by the fund of Science & Technology Bureau of Jilin Province of China (No. 20090320) and the Ministry of Science and Technology of China (No. 2009GJB10042).

REFERENCES

1. Chandra, R.; Rustgi, R. *Prog. Polym. Sci.* **1998**, *23*, 1273.
2. Bogaert, J. C.; Coszach, P. h. *Macromol. Symp.* **2000**, *153*, 287.
3. Drumright, R. E.; Gruber, P. R.; Henton, D. E. *Adv. Mater.* **2000**, *12*, 1841.
4. Guo, X. D.; Zhang, L. J.; Qian, Y.; Zhou, J. *Chem. Eng. J.* **2007**, *131*, 195.
5. Park, Y. J.; Nam, K. H.; Ha, S. J.; Pai, C. M.; Chung, C. P.; Lee, S. J. *J. Control. Release* **1997**, *43*, 151.
6. Edlund, U.; Albertsson, A.C. *J. Bioact. Comp. Polym.* **2000**, *15*, 214.
7. Chen, C.; Lv, G.; Pan, C.; Song, M.; Wu, C.; Guo, D. *Biomed. Mater.* **2007**, *2*, L1.
8. He, C. L.; Huang, Z. M.; Han, X. J.; Liu, L.; Zhang, H. S.; Chen, L. S. *J. Macromol. Sci. B: Phys.* **2006**, *45*, 515.
9. Tomihata, K.; Suzuki, M.; Tomita, N. *Biomed. Mater. Eng.* **2005**, *15*, 381.
10. Greiner, S.; Kadow-Romacker, A.; Wildermann, B.; Schwabe, P.; Schmidmaier, G. *J. Biomed. Mater. Res. A* **2007**, *83A*, 1184.
11. Wildemann, B.; Lubberstedt, M.; Haas, N. P.; Raschke, M. *Biomaterials* **2004**, *25*, 3639.
12. Bergsma, J. E.; Rozena, F. R.; Boering, G.; Debruijn, W. C.; Pennings, A. J. *J. Biomater. Biomed. Mater. Res.* **1995**, *29*, 173.
13. Auras, R. A.; Singh, S. P.; Singh, J. J. *Pack. Technol. Sci.* **2005**, *18*, 207.
14. Auras, R. A.; Harte, B.; Selke, S.; Hernandez, R. J. *Plast. Film Sheet* **2003**, *19*, 123.
15. Zhu, Z. X.; Xiong, C. D.; Zhang, L. L.; Yuan, M. L.; Deng, X. M. *Eur. Polym. J.* **1999**, *35*, 1821.
16. Tasaka, F.; Miyazaki, H.; Ohya, Y.; Ouchi, T. *Macromolecules* **1999**, *32*, 6386.
17. Kim, J. K.; Park, D. J.; Lee, M. S.; Ihn, K. J. *Polym.* **2001**, *42*, 7429.
18. Chen, X. H.; Gross, R. A. *Macromolecules* **1999**, *32*, 308.
19. Lu, J. M.; Qiu, Z. B.; Yang, W. T. *Polymer* **2007**, *48*, 4196.

20. Furukawa, T.; Sato, H.; Murakami, R.; Zhang, J.; Duan, Y. X.; Noda, I.; Ochiai, S.; Ozaki, Y. *Macromolecules* **2005**, *38*, 6445.
21. Shibata, M.; Inoue, Y.; Miyoshi, M. *Polymer* **2006**, *47*, 3557.
22. Tsuji, H.; Ishka, T. *Int. J. Biol. Macromol.* **2001**, *29*, 83.
23. Na, Y. H.; Heiza, Y.; Shuai, X.; Kikkawa, Y.; Doi, Y.; Inoue, Y. *Biomacromolecules* **2002**, *3*, 1179.
24. Yang, J. M.; Chen, H. L.; Yu, J. W.; Hwang, J. C. *Polymer* **1997**, *29*, 657.
25. Liu, T. Y.; Lin, W. C.; Yang, M. C.; Chen, S. Y. *Polymer* **2005**, *46*, 1258.
26. Hu, Y.; Rogunova, M.; Topolkaev, V.; Hiltner, A.; Baer, E. *Polymer* **2003**, *44*, 5701.
27. Hu, Y.; Hu, Y. S.; Topolkaev, V.; Hiltner, A.; Baer, E. *Polymer* **2003**, *44*, 5711.
28. Wu, S. *Polymer* **1985**, *26*, 1855.
29. Wu, S. J. *Appl. Polym. Sci.* **1988**, *35*, 549.
30. Irani, R. R.; Callis, C. F. New York: Wiley; **1963**.
31. Liu, Z. H.; Zhang, X. D.; Zhu, X. G.; Qi, Z. N.; Wang, F. S. *Polymer* **1997**, *38*, 5269.